Physiological and Molecular Plant Pathology 146 (2026) 103441

Contents lists available at ScienceDirect

Physiological and Molecular Plant Pathology

journal homepage: www.elsevier.com/locate/pmpp

Genome-guided production of antifungal metabolites by *Streptomyces philanthi* RM-1-138 from agro-industrial wastes for biological control of phytopathogenic fungi

Wanida Petlamul [a], Sawai Boukaew [a,*], Benjamas Cheirsilp [b], Siriporn Yossan [c], Kanokphorn Sangkharak [d]

[a] Faculty of Agricultural Technology, Songkhla Rajabhat University, Songkhla, 90000, Thailand
[b] Center of Excellence in Innovative Biotechnology for Sustainable Utilization of Bioresources, Faculty of Agro-Industry, Prince of Songkla University, Hatyai, 90110, Thailand
[c] Division of Environmental Science, Faculty of Liberal Arts and Science, Sisaket Rajabhat University, Sisaket, 33000, Thailand
[d] Faculty of Agricultural Technology, Phuket Rajabhat University, Phuket, 83000, Thailand

ARTICLE INFO

Keywords:
Antifungal metabolites
Genome-guided discovery
Biosynthetic gene clusters
LC–QTOF–MS
Oxidative stress

ABSTRACT

Agro-industrial wastes, including palm oil mill effluent (POME) and tuna condensate, represent underutilized substrates for sustainable production of bioactive metabolites. Here, *Streptomyces philanthi* RM-1-138 was evaluated as a genome-guided biocatalyst for antifungal metabolite production against phytopathogenic fungi. Whole-genome sequencing revealed a 6.53 Mb high-GC genome (72.43%) with 30 biosynthetic gene clusters (BGCs), indicating substantial secondary metabolic potential. Optimization of culture conditions (C:N ratio 25:1, 25% substrate) enhanced antifungal activity, achieving 75.8% inhibition of *Schizophyllum commune* and antifungal activity against multiple phytopathogenic fungi. In an oil palm seed model, culture filtrates reduced disease incidence from 76.6% to 39.2% (48.8% disease control), comparable to commercial fungicides. LC–QTOF–MS profiling revealed a chemically diverse metabolite profile and provided putative support for genome-predicted biosynthetic potential. Mechanistic analyses suggest that antifungal activity may involve oxidative stress induction, disruption of fungal antioxidant defenses, and possible utilization of fungal biomass. These findings indicate that RM-1-138 employs a multifactorial, metabolite-associated antifungal strategy and highlight its potential for sustainable waste valorization and biological control of fungal plant diseases.

1. Introduction

Thailand is one of the world's leading producers and exporters of palm oil, generating substantial amounts of agro-industrial by-products, particularly palm oil mill effluent (POME). POME is a high-strength organic wastewater rich in carbohydrates, proteins, lipids, and minerals, making it a promising substrate for microbial cultivation [1]. However, if discharged without proper treatment, POME can cause serious environmental problems, including water pollution, oxygen depletion, and greenhouse gas emissions due to its high organic load [2]. These challenges highlight the need for sustainable strategies to manage and valorize POME.

The conversion of POME into value-added products has therefore attracted increasing attention. Its nutrient-rich composition enables its use as a low-cost medium for microbial growth and the production of bioactive compounds, including enzymes, biosurfactants, biofuels, and antimicrobial metabolites [3,4]. Such waste-to-value approaches offer dual benefits by reducing environmental impact while generating economically valuable products.

In parallel, the seafood processing industry generates large quantities of organic waste, particularly from tuna processing. Tuna condensate, a liquid by-product generated during steaming, is rich in proteins, amino acids, and minerals, making it an attractive nitrogen source for microbial fermentation [5,6]. The combination of carbon-rich POME with nitrogen-rich tuna condensate provides a complementary nutrient profile. This may improve the carbon-to-nitrogen balance, enhance microbial growth, and promote secondary metabolite production. Such integration of agro-industrial wastes represents a promising strategy for

* Corresponding author.
E-mail address: sawai.bo@skru.ac.th (S. Boukaew).

https://doi.org/10.1016/j.pmpp.2026.103441
Received 26 March 2026; Received in revised form 28 July 2026; Accepted 30 July 2026
Available online 1 August 2026

optimizing fermentation performance while promoting circular bioeconomy practices.

Among microbial producers, *Streptomyces* species are well known for their ability to synthesize diverse secondary metabolites, including antibiotics and antifungal compounds [7,8]. These metabolites play important roles in the biological control of plant pathogens and have been widely explored as eco-friendly alternatives to chemical fungicides. In particular, *Streptomyces philanthi* strains have demonstrated strong antifungal activity and the ability to produce bioactive compounds under waste-based cultivation conditions [9–11].

Schizophyllum commune, a wood-decay basidiomycete, has emerged as a pathogen causing seed rot and reduced germination in oil palm, leading to significant economic losses in nursery production [12]. Current management strategies rely largely on chemical fungicides, which may have environmental impacts and contribute to resistance development. Therefore, the development of sustainable, microbially derived antifungal strategies is of considerable interest.

Previous studies have demonstrated that *S. philanthi* strains can grow in various waste-based media, including POME and tuna-derived substrates, and produce metabolites with antifungal activity against several plant pathogens [9–11]. However, these studies have primarily focused on cultivation performance and bioactivity, while the underlying biosynthetic potential and genetic basis of metabolite production remain largely unexplored. In particular, genome-level information for *S. philanthi* RM-1-138 has not been previously reported, limiting our understanding of its secondary metabolite capacity. Moreover, the integration of agro-industrial waste streams with complementary nutrient profiles, such as POME and tuna condensate, has not been systematically evaluated for enhancing metabolite diversity and antifungal efficacy.

Despite increasing research on waste-based fermentation and microbial antifungal metabolites, studies integrating genome mining, metabolite profiling, and mechanistic interpretation remain limited. A comprehensive understanding of how biosynthetic gene clusters are translated into metabolite production and antifungal activity is essential for the rational development of microbial biocontrol systems.

Therefore, this study aims to develop a waste-based cultivation system using a combination of POME and tuna condensate for antifungal metabolite production by *S. philanthi* RM-1-138. Specifically, the objectives were to (i) develop and evaluate mixed agro-industrial substrates for microbial growth and antifungal activity, (ii) assess antifungal efficacy against *S. commune* and other phytopathogenic fungi, (iii) compare the performance of culture filtrates with commercial fungicides, and (iv) integrate genome mining and metabolite profiling to elucidate the potential mechanisms underlying antifungal activity. This work provides a genome-informed and metabolite-driven framework for sustainable waste valorization and biological control of fungal plant diseases.

2. Materials and methods

2.1. Sources of materials

2.1.1. Microorganisms and inoculum preparation

The antagonistic strain *Streptomyces philanthi* RM-1-138, originally isolated by Boukaew et al. [13], was cultured on GYM agar medium composed of 0.4% glucose, 0.4% yeast extract, and 1.0% malt extract, and incubated at 30°C for 10 days before experimental use.

The brown germ and seed rot pathogen of oil palm, *Schizophyllum commune*, was isolated from defective, rotten, and abnormally germinated oil palm seeds [14]. *Rhizoctonia solani* (AG-1 IA) was obtained from the Phatthalung Rice Research Center, while the fruit rot pathogen *Lasiodiplodia theobromae* [15] was isolated from infected nutmeg (*Myristica fragrans*) fruits. *Peniophora salaccae* was isolated from snake fruit rot (*Salacca zalacca*) [16]. *Curvularia oryzae*, causing severe diseases in oil palm, was obtained from the Suratthani Oil Palm Research Center. Aflatoxin-producing *Aspergillus parasiticus* TISTR 3276 and *A. flavus* PSRDC-4 were sourced from Prince of Songkla University and the Phitsanulok Seed Research and Development Center, respectively. *Sclerotium rolfsii*, *Corynespora casiicola*, and *Fusarium incarnatum* were provided by Professor Dr. Sophon Boonlue (Mycorrhiza and Mycotechnology Laboratory, Khon Kaen University) and Professor Dr. Anurag Sunpapao (Agricultural Innovation and Management Division, Prince of Songkla University), respectively.

2.1.2. Palm oil mill effluent and tuna condensate

Palm oil mill effluent (POME) was obtained from Satun Palm Oil Industry Co., Ltd., La-ngu, Satun Province, Thailand, and stored at −20°C until use. Tuna condensate, sourced from Chotiwat Manufacturing Public Co., Ltd., Hatyai, Songkhla Province, Thailand, was also stored at −20°C until use. Both materials were filtered through cheesecloth prior to use.

2.1.3. Commercial fungicides

A total of twelve commercial fungicides were used in this study, including: thiram (80% WG), propiconazole (25% w/v), azoxystrobin (25% w/v), prochloraz (45% w/v), metalaxyl (25% WP), carbendazim (50% w/v), difenoconazole + propiconazole (15% + 15% w/v), chlorothalonil + azoxystrobin (50% + 6% w/v), pyraclostrobin (25% w/v), copper hydroxide (77% WP), fosetyl-aluminium (80% WP), and mancozeb (80% WP). All fungicides used in this study are approved for use and commercially available in Thailand. Each fungicide was applied according to the manufacturer's recommended concentration and guidelines. The recommended dosages used in this study, expressed as final concentrations in PDA (ppm), were as follows: thiram (800 ppm), propiconazole (250 ppm), azoxystrobin (250 ppm), prochloraz (675 ppm), metalaxyl (500 ppm), carbendazim (750 ppm), difenoconazole + propiconazole (300 ppm), chlorothalonil + azoxystrobin (560 ppm), pyraclostrobin (250 ppm), copper hydroxide (1540 ppm), fosetyl-aluminium (2000 ppm), and mancozeb (1200 ppm).

2.1.4. Germinated oil palm seed samples

Germinated oil palm seeds (Tenera hybrid, cv. Golden Tenera Cativa) with radicles about 2 cm long were obtained from Golden Tenera Public Company Limited, Mueang District, Krabi Province, Thailand. The seeds were disinfected by soaking in 2% (v/v) sodium hypochlorite for 3 min, then rinsed three times with sterile distilled water. After sterilization, they were air-dried in a laminar flow cabinet for 30 min under sterile conditions.

2.2. Analytical characteristics of POME and tuna condensate

The chemical characteristics of POME and tuna condensate were analyzed, including chemical oxygen demand (COD), total solids (TS), total suspended solids (TSS), total volatile solids (VS), total volatile suspended solids (VSS), and total phosphorus (TP), following standard methods [17]. Total Kjeldahl Nitrogen (TKN) and total protein were determined using the Kjeldahl method [17] and an N/protein analyzer, respectively. Magnesium (Mg), total phosphate, and ammonium-nitrogen (NH_4-N) were measured using an Inductively Coupled Plasma–Optical Emission Spectrometer (ICP–OES). Chloride and salinity were determined using photometric methods and a salinity meter, respectively. The pH was measured with a pH meter.

Glucose, xylose, and arabinose were quantified by high-performance liquid chromatography (HPLC; Agilent 1200 series) equipped with an Aminex HPX-87H (300 mm × 7.8 mm) ion exclusion column (Bio-Rad, Hercules, CA) and a refractive index (RI) detector. Samples were diluted with HPLC-grade deionized water, filtered through a 0.22 μm, 13 mm Nylon membrane filter (Sartorius, Goettingen, Germany), and injected into the chromatograph under the following conditions: column temperature of 65°C, 5 mM sulfuric acid as the mobile phase at a flow rate of 0.6 mL/min, and an injection volume of 20 μL. Concentrations were

Table 1
Characteristics of raw materials (tuna condensate and palm oil mill effluent, POME) used for the production of antifungal compounds by *S. philanthi* RM-1-138.

Parameter	Unit	Tuna condensate	POME
pH		5.89	4.52
Total nitrogen (TKN)	mg/L	6800 ± 170	1250 ± 37
Total protein	% (w/w)	4.15 ± 0.10	0.72 ± 0.02
Chemical oxygen demand COD	mg/L	54,950 ± 137	69,350 ± 173
Total phosphorus	mg/L	59.13 ± 147	17.33 ± 43
Ammonium-nitrogen (NH_4-N)	mg/L	20 ± 0.5	80 ± 2.0
Total Phosphate	mg/L	2580 ± 64.5	756 ± 18.9
Chloride	mg/L	10,600 ± 265	4000 ± 89
Magnesium (Mg)	mg/L	2596 ± 64	6794 ± 169
Salinity	ppt	19.15 ± 0.48	7.23 ± 0.21
Total solids (TS)	mg/L	66,038 ± 819	59,933 ± 134
Total Volatile (VS)	mg/L	55,728 ± 194	49,860 ± 536
Total suspended solids (TSS)	mg/L	750 ± 28	26,620 ± 501
Total Volatile suspended solids (VSS)	mg/L	912 ± 3.6	24,180 ± 424
Glucose	g/L	0.80 ± 0.02	4.22 ± 0.21
Xylose	g/L	0.24 ± 0.02	3.07 ± 0.05
Arabinose	g/L	ND	0.34 ± 0.04

Note: Values are expressed as mean ± SD (n = 3).

Table 2
Genomic features and chromosomal characteristics of *S. philanthi* RM-1-138.

Feature	Value
Genome size (Mb)	6.53
GC content (%)	72.43
Number of contigs	641
Contig N50 (bp)	18,383
Sequencing depth (×)	142.2
BUSCO completeness (%)	94.8
BUSCO fragmented (%)	2.5
BUSCO missing (%)	2.7
Number of CDSs	5855
Number of tRNA genes	85
Number of rRNA genes	3
Average gene length (bp)	904
Secondary metabolite biosynthetic gene clusters	30

calculated using calibration curves generated from standard solutions [18]. All experiments were conducted using three independent biological replicates (n = 3), each with three technical replicates per treatment.

2.3. Genome sequencing and annotation of *S. philanthi* RM-1-138

The whole genome of *S. philanthi* RM-1-138 was sequenced using an Illumina sequencing platform. Clean reads were *de novo* assembled using Unicycler in short-read assembly mode [19]. Gene prediction and genome annotation were conducted using PROKKA for protein-coding sequences (CDSs), tRNAscan-SE v2.0 for transfer RNA (tRNA) genes, and Barrnap for ribosomal RNA (rRNA) gene identification [20].

Biosynthetic gene clusters (BGCs) associated with secondary metabolite production were predicted using antiSMASH v6.0.1. The identified BGCs were annotated and compared with experimentally characterized clusters deposited in the MIBiG database. Percent similarity values were assigned based on concordance in gene content, synteny, and overall cluster architecture as defined by the antiSMASH output.

2.4. Antagonistic activity of *S. philanthi* RM-1-138 against *S. commune*

In vitro confrontation assays were conducted according to Mannaa et al. [21], with slight modifications. A loopful of *S. philanthi* RM-1-138 was streaked onto PDA plates and incubated at 30°C for 10 days. After the pre-incubation period, a 5-mm mycelial plug from a 3-day-old *S. commune* colony was inoculated either on the opposite side of the plate (setup I) or at the center between two streaks of RM-1-138 (setup II). Plates inoculated with *S. commune* alone served as the control. All plates were incubated at 28 ± 2°C for 5 days. Colony diameters were measured, and the percentage of mycelial growth inhibition was calculated according to Boukaew et al. [13] as follows: Percentage of inhibition (%) = [(Control − Treatment)/Control] × 100. All experiments were conducted using three independent biological replicates (n = 3), each with three technical replicates per treatment.

2.5. Optimization of C:N ratios in tuna condensate and POME for antifungal metabolite production by *S. philanthi* RM-1-138 against *S. commune*

2.5.1. Medium preparation

Culture media were prepared to optimize C:N ratios in POME and tuna condensate for enhanced growth of *S. philanthi* RM-1-138 and production of antifungal metabolites against *S. commune*. POME served as the carbon source and tuna condensate as the nitrogen source, based on their biochemical composition. C:N ratios of 20:1, 25:1, 30:1, and 35:1 were tested. For each ratio, four effluent concentrations were prepared: 100% (undiluted), 75%, 50%, and 25%, diluted with sterile distilled water. The initial pH of all media was adjusted to 7.0 and sterilized by autoclaving at 121°C for 15 min.

2.5.2. Preparation of seed culture and inoculation

A seed culture of *S. philanthi* RM-1-138 was prepared by submerged cultivation in GYM broth (100 mL in 250 mL flasks) at 28 ± 2°C on a rotary shaker (150 rpm), with the medium adjusted to pH 7.0 prior to autoclaving. After 3 days, 5 mL aliquots were transferred into fresh GYM broth (100 mL) and incubated for another 3 days. The culture was centrifuged (5000 × g, 15 min), the supernatant discarded, and the pellet resuspended in sterile distilled water and adjusted to 10^7 CFU/mL.

The seed suspension (5% v/v) of the strain RM-1-138 was inoculated into the medium prepared as described in section 2.5.1. Immediately after inoculation, a 1 mL aliquot was collected as the time-zero sample for the determination of initial COD. The cultures were then incubated on a rotary shaker at 150 rpm for 10 days. Upon completion of the cultivation period, the broth was evenly divided into two portions: one portion was used for COD measurement, while the other was subjected to antifungal activity assays.

2.5.3. COD measurement and antifungal assay

COD was analyzed according to APHA standard methods [16]. The COD removal efficiency (%) was calculated as follows: COD removal efficiency (%) = [($COD_{(initial)}$ − $COD_{(final)}$)/$COD_{(initial)}$] × 100. Experiments were performed in three independent biological replicates (n = 3), each consisting of three technical replicates per treatment.

For antifungal activity, the culture broth was first filtered through filter paper, then centrifuged at 5000 × g for 15 min, and finally passed through a 0.22 μm Millipore membrane to obtain culture filtrates (CFs). Each CF was mixed with sterile PDA at a 1:1 ratio (5 mL CFs + 5 mL PDA; final volume 10 mL). PDA mixed with the optimized medium (without inoculum) at the same ratio served as the control. A 5-mm mycelial plug from a 3-day-old.

S. commune colony was placed at the center of each plate, and the cultures were incubated at 28 ± 2°C for 5 days. Colony diameters were measured, and the percentage of inhibition was calculated as described above. All experiments were conducted using three independent biological replicates (n = 3), each with three technical replicates per treatment.

Table 3
Prediction of biosynthetic gene clusters (BGCs) of secondary metabolites in *S. philanthi* RM-1-138 using antiSMASH v6.0.1.

Region	Type	From	To	Most similar known cluster	BGC/Metabolite class	Similarity (%)
Region 2.1	CDPS, arylpolyene	1	53,383	hygromycin A	Saccharide	93%
Region 5.1	NRPS,T1PKS	9839	60,286	bacillibactin	NRP	38%
Region 6.1	T1PKS	8599	56,098			
Region 9.1	NRPS-like	22,615	49,436	sporolide A/sporolide B	NRP + Polyketide:Enediyne type I	21%
Region 13.1	NAPAA, butyrolactone	13,990	45,550	lactonamycin	Polyketide	3%
Region 21.1	terpene	2053	24,299	geosmin	Terpene	100%
Region 25.1	T2PKS	1	32,514	spore pigment	Polyketide	66%
Region 45.1	NRPS	1	25,613	paromomycin	Saccharide	10%
Region 59.1	PKS-like, butyrolactone	1	24,986	kirromycin	NRP + Polyketide:Modular type I + Polyketide: Trans-AT type I	3%
Region 71.1	NRPS-like,NRPS	1	23,338	anisomycin	Other	53%
Region 73.1	butyrolactone	15,809	23,136			
Region 76.1	other	1	22,945			
Region 82.1	RiPP-like	1	9254			
Region 96.1	lanthipeptide-class-i	1	18,822	mycotrienin I	NRP + Polyketide	7%
Region 109.1	NRPS	1	18,516			
Region 130.1	terpene	1	16,313	5-isoprenylindole-3-carboxylate β-D-glycosyl ester	Other	14%
Region 135.1	ectoine	2443	12,847	ectoine	Other	100%
Region 136.1	terpene	1	15,720	hopene	Terpene	46%
Region 146.1	T3PKS	1	14,635	herboxidiene	Polyketide	2%
Region 155.1	ectoine	1544	11,930	netropsin	NRP	13%
Region 161.1	NRPS	1	13,717			
Region 167.1	T1PKS, NRPS	1	13,237	rakicidin A/rakicidin B	NRP:Cyclic depsipeptide + Polyketide:Modular type I	44%
Region 174.1	NRPS-like	1	12,638			
Region 175.1	blactam	1	12,511	valclavam/(−)-2-(2-hydroxyethyl) clavam	Other:Non-NRP beta-lactam	57%
Region 179.1	siderophore	2775	12,166			
Region 180.1	terpene	1	10,979	ebelactone	Polyketide	5%
Region 197.1	NRPS	1	11,103			
Region 239.1	T1PKS	1	9283			
Region 413.1	arylpolyene, ladderane	1	3973	atratumycin	NRP	10%
Region 624.1	T1PKS	1	1070			

2.6. Effect of seed inoculum size of S. philanthi RM-1-138 on antifungal metabolite production against S. commune

The effect of seed inoculum size of RM-1-138 in the optimized medium (C:N = 25:1, 25% diluted) on antifungal metabolite production against *S. commune* was investigated. Seed inoculum sizes of 1%, 2%, 5%, 10%, and 15% (v/v) were inoculated into the optimized medium. Immediately after inoculation, 1 mL of broth culture was collected as a time-zero sample for initial COD determination. The cultures were incubated on a rotary shaker (150 rpm) at 28 ± 2°C for 10 days. At the end of cultivation, the broth was divided into two portions: one for COD measurement and the other for antifungal activity assays, as described above.

For the antifungal assay, each CF was combined with sterile PDB in a 1:1 proportion (10 mL CFs + 10 mL PDB; total volume 20 mL). The control treatment consisted of PDB mixed with the uninoculated optimized medium in the same ratio. Subsequently, a 5-mm mycelial disc obtained from a 3-day-old *S. commune* culture was transferred into each flask and incubated on a rotary shaker at 150 rpm and 28 ± 2°C for 5 days. After incubation, the fungal biomass was harvested using pre-weighed dried filter paper, oven-dried at 60°C for 3 days, and weighed. Mycelial growth inhibition was calculated as previously described. All experiments were conducted using three independent biological replicates (n = 3), each with three technical replicates per treatment.

2.7. Effect of different concentrations of antifungal metabolites produced by S. philanthi RM-1-138 in optimized medium on the inhibition of S. commune

The CFs of *S. philanthi* RM-1-138 were prepared as described above and sterilized by filtration through a 0.22 μm membrane filter before use. To evaluate the antifungal activity at different concentrations, culture filtrates were incorporated into molten sterile double-strength PDA, which was used to compensate for dilution and maintain nutrient concentrations equivalent to those of standard PDA. Final CFs concentrations of 10%, 15%, 30%, 45%, and 60% (v/v) were prepared by adjusting the total medium volume to 10 mL per Petri dish. In the control treatment, PDA without CFs was used. A 5-mm mycelial plug taken from a 3-day-old culture of *S. commune* was placed at the center of

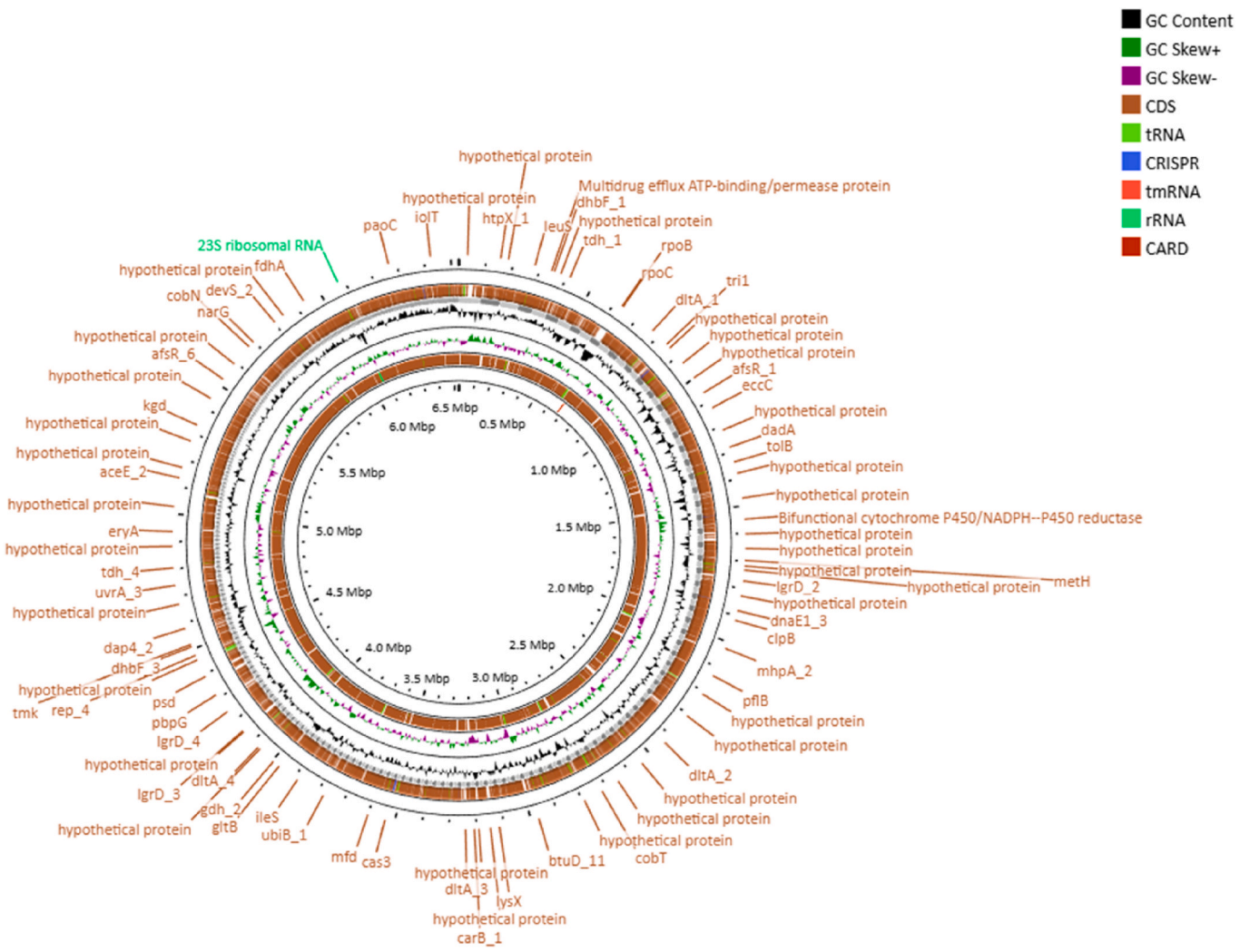

Fig. 1. The map of the complete chromosome of *S. philanthi* RM-1-138.

each Petri dish. Plates were incubated at 28 ± 2°C for 5 days. Colony diameters were measured, and percentage inhibition was calculated as described previously. All experiments were conducted using three independent biological replicates (n = 3), each with three technical replicates per treatment.

2.8. Comparative evaluation of the in vitro antifungal efficacy of S. philanthi RM-1-138 culture filtrates and commercial fungicides

The antifungal activity of RM-1-138 CFs from the optimized medium was compared with twelve commercial fungicides—thiram, propiconazole, azoxystrobin, prochloraz, metalaxyl, carbendazim, difenoconazole + propiconazole, chlorothalonil + azoxystrobin, pyraclostrobin, copper hydroxide, fosetyl-aluminium, and mancozeb—against *S. commune* on PDA. Each fungicide was incorporated into sterile PDA at its recommended final concentrations (ppm) as described in Section 2.1.3. The control treatment did not receive any application of CFs or fungicide. A 5-mm mycelial plug from a 3-day-old *S. commune* culture was placed at the center of each plate. Plates were incubated at 28 ± 2°C for 5 days. Colony diameters were recorded, and inhibition (%) was calculated as described above. All experiments were conducted using three independent biological replicates (n = 3), each with three technical replicates per treatment.

2.9. Antifungal activity of S. philanthi RM-1-138 culture filtrates against multiple plant pathogenic fungi

The antifungal activity of RM-1-138 CFs from the optimized medium was evaluated against nine phytopathogenic fungi: *R. solani*, *L. theobromae*, *P. salaccae*, *C. oryzae*, *A. parasiticus*, *A. flavus*, *S. rolfsii*, *C. cassiicola*, and *F. incarnatum* in PDB. The CFs were mixed with sterile PDB at a 1:1 ratio (10 mL filtrate + 10 mL PDB; final volume 20 mL). In the control treatment, no CFs were applied. A 5-mm mycelial plug from a 3-day-old colony was inoculated into each flask for *R. solani*, *L. theobromae*, *P. salaccae*, *C. oryzae*, *S. rolfsii*, *C. cassiicola*, and *F. incarnatum*. For *A. parasiticus* TISTR 3276 and *A. flavus* PSRDC-4, 50 μL of a spore suspension (10^7 spores/mL) was added to each flask. All cultures were incubated at 28 ± 2°C on a rotary shaker (150 rpm) for a duration depending on the growth rate of each pathogen. Mycelial mats were collected on pre-weighed filter paper, dried at 60°C for 3 days, and weighed. The percentage of growth inhibition was calculated as described above. All experiments were conducted using three independent biological replicates (n = 3), each with three technical replicates per treatment.

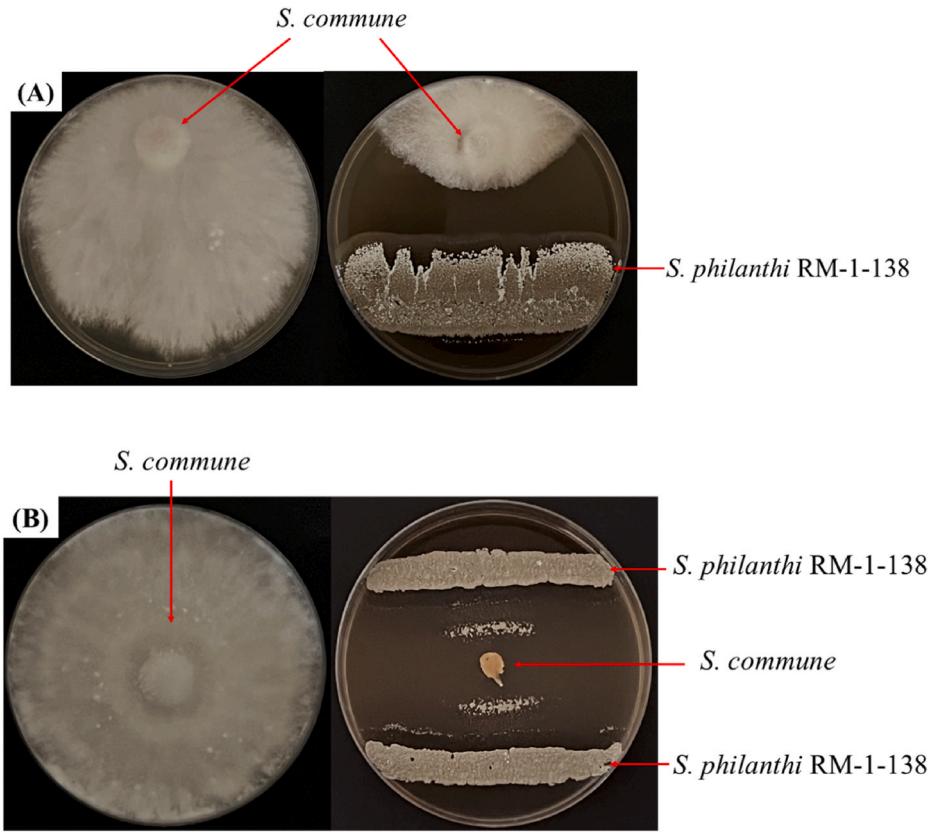

Fig. 2. Antifungal activity of *S. philanthi* RM-1-138 against *S. commune* evaluated using a dual culture assay after 5 days of incubation at 28 ± 2°C. **(A)** Single inoculation of RM-1-138 and **(B)** double inoculum of RM-1-138.

2.10. Comparative assessment of S. philanthi RM-1-138 culture filtrates and commercial fungicides against S. commune infection in an oil palm seed model

The effectiveness of RM-1-138 CFs was compared with four commercial fungicides—propiconazole, difenoconazole + propiconazole, copper hydroxide, and mancozeb—that had previously demonstrated more than 80% inhibition on PDA. Germinated oil palm seeds were surface-sterilized and immersed in either the CFs or fungicide solutions prepared at the manufacturer's recommended concentrations for 10 min. The treated seeds were air-dried, and a 5 mm mycelial disc of *S. commune* was positioned adjacent to the radicle of each seed. For the negative control, seeds were neither inoculated with the pathogen nor treated, while in the positive control, seeds were inoculated with the fungus but received no treatment. All treated and control seeds were placed on sterile metal racks inside sealed plastic containers maintained at 90% relative humidity and incubated at 28 ± 2°C for 20 days. After incubation, the seeds were examined for disease symptoms such as brown discoloration and mycelial coverage on the germ or radicle, indicative of seed rot. Disease incidence was determined according to Petlamul et al. [14] using the following formula: Disease incidence (%) = (Number of infected seeds/Total number of seeds) × 100. All experiments were conducted using three independent biological replicates (n = 3), each consisting of 10 germinated seeds per treatment.

2.11. LC–QTOF–MS-based metabolite profiling of culture filtrates of S. philanthi RM-1-138

Metabolite profiling of culture filtrates produced by *S. philanthi* RM-1-138 grown in the optimized medium was carried out using liquid chromatography coupled with quadrupole time-of-flight mass spectrometry (LC–QTOF–MS). Analyses were performed on an Agilent 1290 Infinity II ultra-high-performance liquid chromatography (UHPLC) system interfaced with an Agilent 6545 Q-TOF mass spectrometer (Agilent Technologies, USA). Culture filtrate samples were prepared following the same procedure described for antifungal activity assays and were subjected to LC–MS analysis without further modification. Chromatographic separation was achieved on a Zorbax Eclipse Plus C18 Rapid Resolution HD column (150 × 2.1 mm, 1.8 μm particle size), which was maintained at 25°C throughout the analysis. The mobile phase comprised water containing 0.1% acetic acid (solvent A) and LC–MS–grade methanol (solvent B), delivered at a constant flow rate of 0.2 mL/min. The gradient program was initiated with 95% solvent A for 2 min, followed by a gradual decrease to 0% solvent A over 40 min. This composition was maintained until 45 min before re-equilibration to the initial conditions. A sample volume of 10 μL was injected for each run.

Mass spectrometry was performed in both positive (+ESI) and negative (−ESI) electrospray ionization modes using automated data-dependent MS/MS acquisition (AutoMS/MS). Full-scan MS spectra were acquired over an m/z range of 100–1200, while MS/MS spectra were collected in the range of m/z 50–1200 with stepped collision energies of 10, 20, and 40 V. Continuous internal mass calibration was applied using reference ions at m/z 121.0509 and 922.0098 for positive ion mode and m/z 112.9856 and 1033.9881 for negative ion mode to ensure mass accuracy. Putative annotation of detected metabolites was performed based on accurate mass measurements and MS/MS fragmentation patterns by comparison with the METLIN metabolite database using MassHunter PCD/PCDL software (version 8.0, Agilent Technologies). The resulting metabolite annotations were therefore considered putative (MSI levels 2–3), as identification was not confirmed using authentic reference standards or retention time matching.

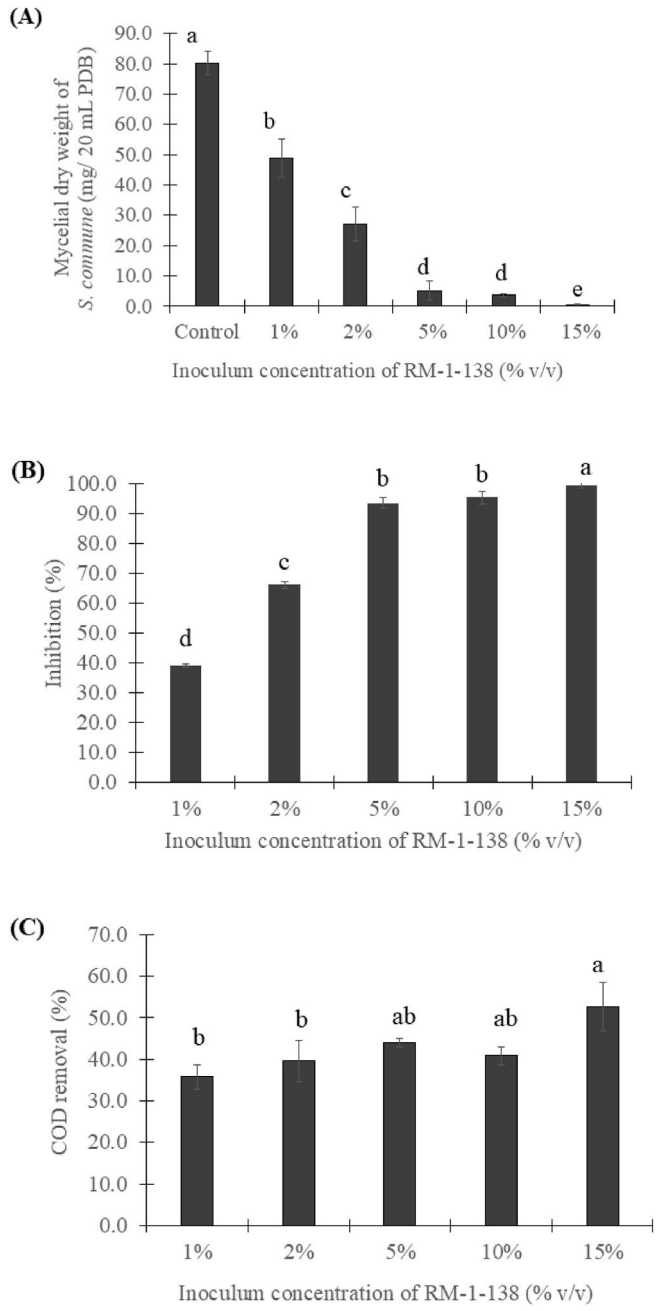

Fig. 3. Effect of seed inoculum size (1% to 15% v/v) of *S. philanthi* RM-1-138 on **(A)** mycelial growth, **(B)** inhibition percentage of *S. commune* after 5 days of incubation at 28 ± 2°C, and **(C)** COD removal. Data are presented as mean ± SD (n = 3). Bars sharing the same letter are significantly different (Tukey's HSD test, $p < 0.05$).

2.12. Mycolytic assay and interaction analysis of S. philanthi RM-1-138 against S. commune

To evaluate potential interactions between *S. philanthi* RM-1-138 and *S. commune*, including possible utilization of fungal biomass, several *in vitro* assays were performed.

2.12.1. Mycolytic assay

The ability of RM-1-138 to utilize *S. commune* mycelial biomass was assessed using a mycolytic assay [21,22]. Fungal biomass was produced by cultivating *S. commune* in PDB at 28 ± 2°C with continuous agitation at 150 rpm for 48 h. After incubation, the fungal mycelia were aseptically harvested, rinsed twice with sterile distilled water to remove residual extracellular compounds, and weighed.

The bacterial inoculum was prepared from 3-day-old cultures and adjusted to an optical density of 0.6 at 600 nm (OD600). The assay was carried out in GYM medium diluted 1000-fold (v/v) with sterile distilled water. Two experimental setups were established: bacterial cultures supplemented with fungal mycelia (+fungi) and bacterial cultures without fungal material (−fungi). Each 3-mL reaction mixture contained 6 mg of fungal biomass and 100 µL of bacterial suspension. Cultures were incubated at 28 ± 2°C with shaking at 150 rpm for 3 days. Bacterial growth was quantified by viable plate counts (CFU determination). Aliquots (200 µL) from serial dilutions were plated onto GYM agar and incubated for 48 h at 28 ± 2°C before enumeration. All experiments were conducted using three independent biological replicates (n = 3), each with three technical replicates per treatment.

2.12.2. Oxidative stress–related assays

Oxidative stress–related parameters in *S. commune* were analyzed following exposure to CFs of *S. philanthi* RM-1-138. Actively growing mycelia of *S. commune* were obtained by transferring a 5-mm agar plug from the colony margin of a 3-day-old culture into 100 mL of PDB. Cultures were incubated at 28 ± 2°C with shaking at 150 rpm for 3 days to allow sufficient mycelial development. After incubation, the mycelial biomass was collected, rinsed with sterile distilled water, and weighed. One gram (fresh weight) of washed mycelia was transferred into 10 mL of PDB supplemented with 60% (v/v) CFs of RM-1-138. Control samples contained PDB without CFs supplementation. All treatments were incubated under identical conditions for an additional 3 days.

Following exposure, mycelia from treated and control groups were harvested and processed for biochemical analyses. Samples were homogenized in phosphate-buffered saline (PBS; 100 mM, pH 7.4) and centrifuged at 8000 rpm for 10 min at 4°C. The resulting supernatants were collected for determination of oxidative stress-related parameters.

Intracellular oxidative status was evaluated by measuring reactive oxygen species (ROS), catalase (CAT) activity, superoxide dismutase (SOD) activity, and glutathione redox balance (GSH and GSSG). These parameters are commonly used as indicators of cellular oxidative status in fungi [23,24].

ROS accumulation was assessed using 2′,7′-dichlorodihydrofluorescein diacetate (DCFH-DA), with fluorescence measured at excitation/emission wavelengths of 485/530 nm [25,26]. Catalase activity was determined by monitoring hydrogen peroxide decomposition following Beers and Sizer [27] and expressed as units per minute per milligram protein. Superoxide dismutase activity was measured based on inhibition of quercetin auto-oxidation [28].

For glutathione analysis, samples were extracted in phosphate buffer containing EDTA and metaphosphoric acid. Reduced glutathione (GSH) and oxidized glutathione (GSSG) were quantified fluorometrically following derivatization methods described previously [28]. Total protein content was determined using the Lowry assay [29].

All experiments were conducted using three independent biological replicates (n = 3), each with three technical replicates per treatment.

2.13. Statistical analysis

Data involving multiple treatments were analyzed using one-way analysis of variance (ANOVA), followed by Tukey's Honestly Significant Difference (HSD) test for multiple comparisons at $p < 0.05$. Comparisons between two groups were performed using an independent-samples *t*-test at $p < 0.05$. All statistical analyses were performed using IBM SPSS Statistics version 26 (IBM Corp., Armonk, NY, USA).

Table 4
Effect of different concentrations (1–60% v/v) of *S. philanthi* RM-1-138 culture filtrates (RM-1-138 CFs) in an effluent-based medium under optimized conditions (C:N ratio of 25:1, 25% dilution) on *S. commune* growth on PDA after incubation at 28 ± 2°C for 5 days.

Parameters	Concentrations of RM-1-138 CFs (% v/v)					
	Control	1	15	30	45	60
Radial growth (cm)	$9.00^{a} \pm 0.00$	$8.84^{a} \pm 0.15$	$6.60^{b} \pm 0.21$	$3.70^{c} \pm 0.34$	$2.46^{d} \pm 0.71$	$0.91^{e} \pm 0.04$
Inhibition (%)	-	$1.82^{e} \pm 0.13$	$26.70^{d} \pm 1.34$	$58.90^{c} \pm 1.04$	$72.67^{b} \pm 0.02$	$89.85^{a} \pm 0.05$
Colony morphology						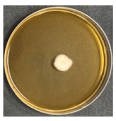

Note: Values are expressed as mean ± SD (n = 3). Means followed by the same letter within each row are significantly different according to Tukey's HSD test (ANOVA, $p < 0.05$).

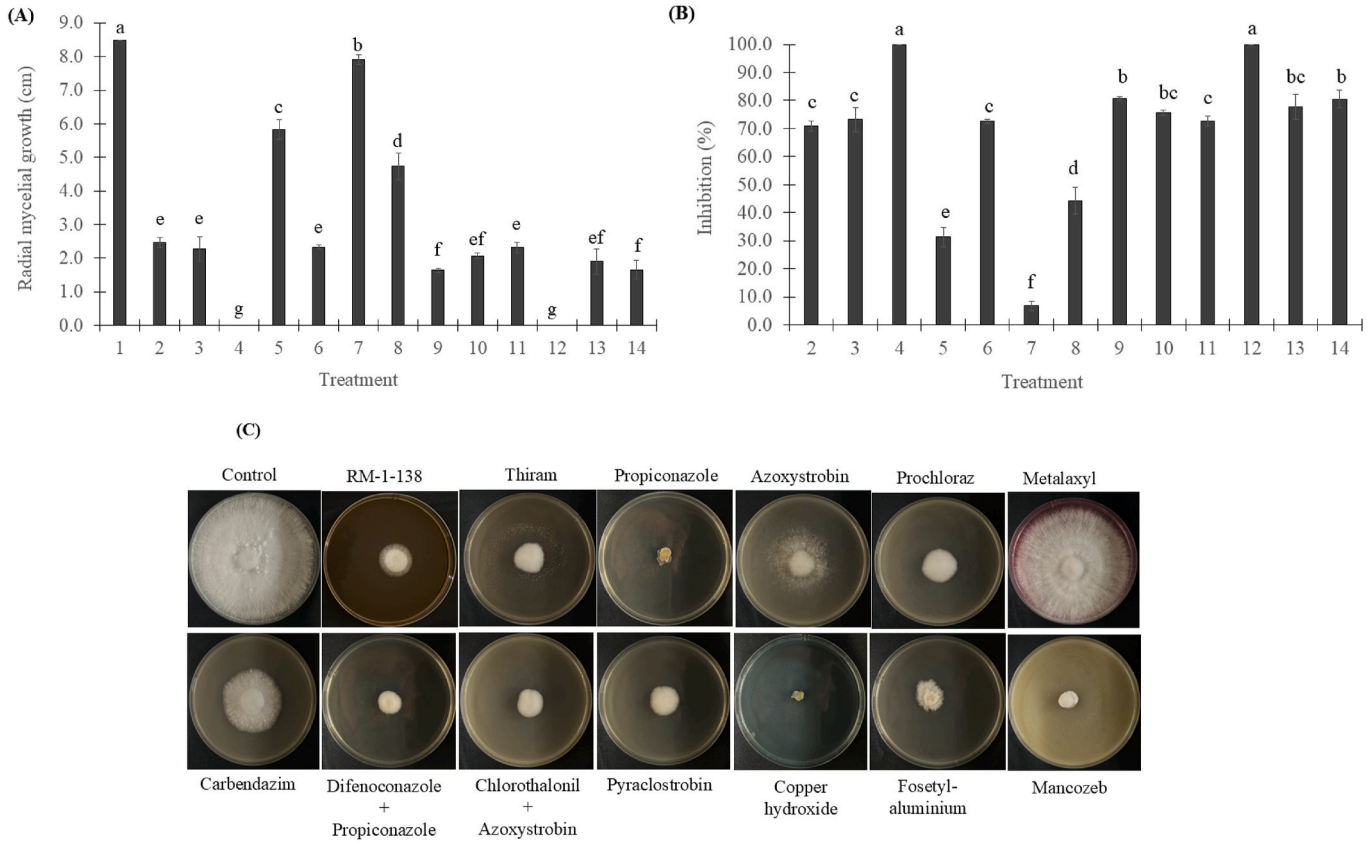

Fig. 4. Comparative antifungal efficacy of *S. philanthi* RM-1-138 culture filtrates from the optimized medium and twelve commercial fungicides on **(A)** radial mycelial growth, **(B)** inhibition percentage, and **(C)** colony morphology of *S. commune* after 5 days of incubation at 28 ± 2°C. Data are presented as mean ± SD (n = 3). Bars sharing the same letter are significantly different (Tukey's HSD test, $p < 0.05$). ***Note:*** (1) Control, (2) RM-1-138 CFs, (3) Thiram, (4) Propiconazole, (5) Azoxystrobin, (6) Prochloraz, (7) Metalaxyl, (8) Carbendazim, (9) Difenoconazole + Propiconazole, (10) Chlorothalonil + Azoxystrobin, (11) Pyraclostrobin, (12) Copper hydroxide, (13) Fosetyl-aluminium, (14) Mancozeb.

3. Results

3.1. Analytical characteristics of POME and tuna condensate

The chemical characteristics of tuna condensate and POME used as substrates for antifungal compound production by *S. philanthi* RM-1-138 are summarized in Table 1. Tuna condensate exhibited a higher pH (5.89) than POME (4.52) and was markedly richer in nitrogenous components, including total Kjeldahl nitrogen (6800 vs. 1250 mg/L) and total protein (4.15% vs. 0.72%). In contrast, POME contained higher levels of chemical oxygen demand (69,350 vs. 54,950 mg/L) and ammonium nitrogen (80 vs. 20 mg/L). Differences in mineral composition were also evident, with tuna condensate having a higher chloride concentration (10,600 mg/L), whereas POME contained greater amounts of magnesium (6794 vs. 2596 mg/L) and exhibited higher salinity (19.15 vs. 7.23 ppt). In terms of solid fractions, tuna condensate showed higher total solids (66,038 mg/L) and volatile solids (55,728 mg/L), while POME was characterized by substantially higher total suspended solids (26,620 mg/L) and volatile suspended solids (24,180 mg/L). The sugar profiles further distinguished the two substrates. POME contained higher concentrations of glucose (4.22 g/L), xylose (3.07 g/L), and arabinose (0.34 g/L), whereas these sugars were present at much lower levels in tuna condensate (0.80 and 0.24 g/L for glucose and xylose, respectively, with arabinose not detected). Collectively, these compositional differences suggest distinct carbon and nitrogen availability between the two substrates, which may play a key

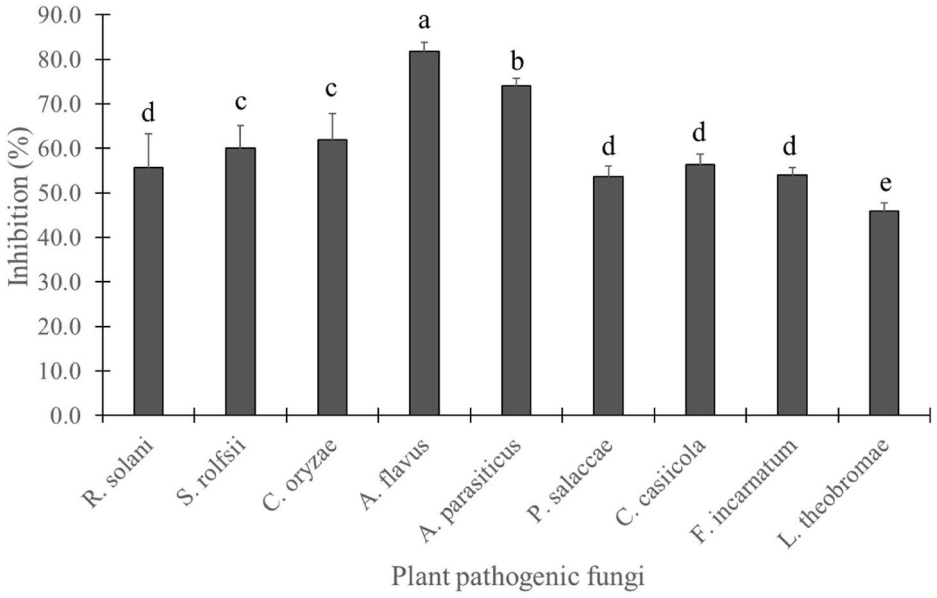

Fig. 5. Antifungal activity of *S. philanthi* RM-1-138 culture filtrates from the optimized medium against multiple plant pathogenic fungi after 3–7 days of incubation at 28 ± 2°C. Data are presented as mean ± SD (n = 3). Bars sharing the same letter are significantly different (Tukey's HSD test, $p < 0.05$).

role in regulating the biosynthesis of antifungal metabolites by *S. philanthi* RM-1-138.

3.2. General genomic features of S. philanthi RM-1-138

Whole-genome sequencing of *S. philanthi* RM-1-138 generated a draft genome assembly of 6.53 Mb with a high GC content of 72.43%, which is characteristic of metabolically versatile *Streptomyces* species (Table 2). The genome assembly was obtained with an average sequencing depth of 142.2×, resulting in 641 contigs with a contig N50 of 18,383 bp. Genome completeness assessment using BUSCO indicated 94.8% complete, 2.5% fragmented, and 2.7% missing BUSCO genes, supporting the overall quality and completeness of the genome assembly (Table 2). The whole-genome shotgun project has been deposited in the GenBank database under the accession number JCANQV000000000.

Genome annotation identified 5855 predicted coding sequences (CDSs) with an average gene length of 904 bp, together with 85 tRNA genes and three rRNA genes, indicating a well-equipped translational system required for active growth and metabolite production. Genome mining using antiSMASH predicted 30 biosynthetic gene clusters (BGCs), highlighting the substantial genetic potential of strain RM-1-138 for secondary metabolite biosynthesis (Table 2). Collectively, these genomic features indicate that *S. philanthi* RM-1-138 possesses considerable metabolic and biosynthetic versatility, supporting its potential as a producer of antifungal compounds.

3.3. Biosynthetic gene cluster analysis of S. philanthi RM-1-138

Genome mining using antiSMASH v6.0.1 identified 30 BGCs distributed across the chromosome of *S. philanthi* RM-1-138, representing a wide range of secondary metabolite classes (Table 3; Fig. 1). These included NRPS, PKS, hybrid NRPS–PKS systems, terpenes, RiPPs, siderophores, and other metabolite-associated clusters, reflecting substantial biosynthetic diversity. Several BGCs exhibited high similarity to well-characterized clusters in the MIBiG database. For example, a terpene cluster (Region 21.1) showed 100% similarity to the geosmin biosynthetic cluster, while an ectoine cluster (Region 135.1) also displayed complete conservation with known reference sequences (Table 3). Additional clusters, including a CDPS/arylpolyene-associated region (Region 2.1), shared high similarity (93%) with the hygromycin A biosynthetic cluster.

In contrast, a large proportion of BGCs displayed low similarity (<20%) to known clusters, including those related to lactonamycin, kirromycin, herboxidiene, mycotrienin I, and atratumycin. Several NRPS- and PKS-containing clusters lacked close homologs in the MIBiG database, suggesting the presence of potentially novel or previously uncharacterized biosynthetic gene clusters that may encode previously uncharacterized secondary metabolites. Hybrid systems were also detected, including NRPS–PKS clusters with moderate to low similarity to rakicidin A/B, sporolide A/B, and kirromycin-associated pathways. Notably, the coexistence of highly conserved clusters and numerous low-similarity BGCs highlights both the functional versatility and the unexplored biosynthetic potential of strain RM-1-138. These genome mining results indicate that RM-1-138 harbors substantial biosynthetic potential. However, experimental characterization is required to identify the metabolites encoded by these predicted gene clusters and to verify their biological activities.

3.4. Antagonistic activity of S. philanthi RM-1-138 against S. commune

The antifungal activity of *S. philanthi* RM-1-138 against the fungal *S. commune* was assessed using a dual culture assay (Fig. 2). *S. philanthi* RM-1-138 was streaked on PDA, and a plug of *S. commune* was placed 1 cm from the opposite edge. Single inoculation of RM-1-138 inhibited *S. commune* growth by 54.07% (Fig. 2A), whereas doubling the RM-1-138 inoculum resulted in complete inhibition (100%) (Fig. 2B).

3.5. Optimization of C:N ratios in tuna condensate and POME for antifungal metabolite production by S. philanthi RM-1-138 against S. commune

The effects of C:N ratio and substrate concentration on antifungal metabolite production by *S. philanthi* RM-1-138 are summarized in Table S1 (Supplementary Data). Culture media formulated from POME (carbon source) and tuna condensate (nitrogen source) revealed a strong interactive effect between nutrient balance and metabolic output. No antifungal activity was detected at high substrate concentrations (100% and 75%) across all C:N ratios, indicating that excessive nutrient availability may suppress secondary metabolite production. At a C:N ratio of 20:1, only moderate inhibition of *S. commune* (35.5%) was

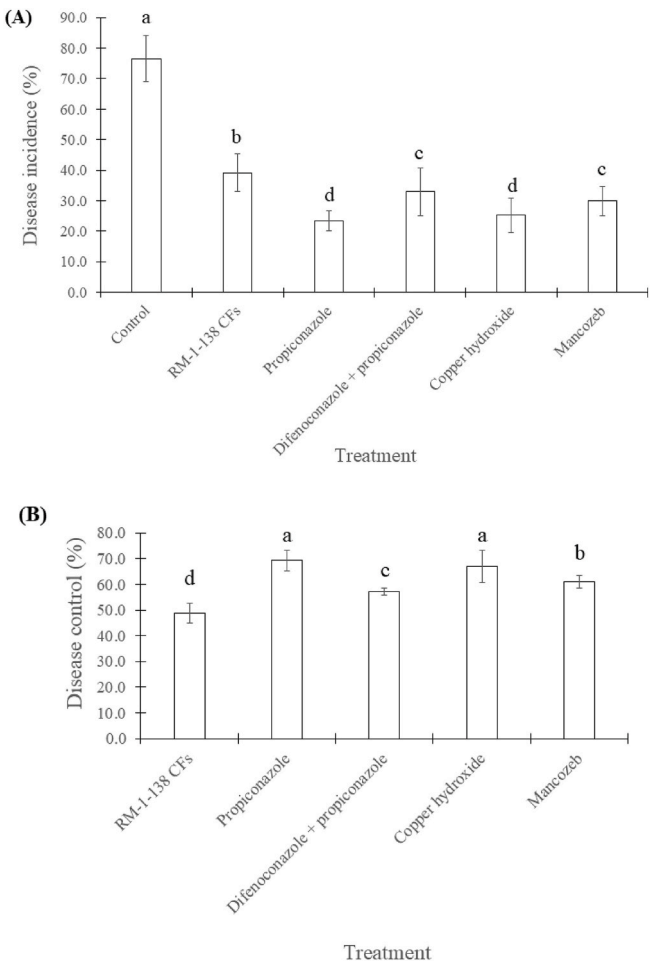

Fig. 6. Efficacy comparison of *S. philanthi* RM-1-138 culture filtrates produced from the optimized medium and four chemical fungicides (propiconazole, difenoconazole + propiconazole, copper hydroxide, and mancozeb) in controlling *S. commune* infection in germinated oil palm seeds after 20 days of incubation at 30°C under humid conditions. **(A)** Disease incidence (%) and **(B)** Disease control (%). Data are presented as mean ± SD (n = 3). Bars sharing the same letter are significantly different (Tukey's HSD test, $p < 0.05$). ***Note:*** Disease incidence was assessed based on the presence of brown discoloration or seed rot symptoms characterized by mycelial growth covering the germ or radicle.

observed at 50% concentration.

In contrast, a C:N ratio of 25:1 markedly enhanced antifungal activity. The highest inhibition (75.8%) was achieved at 25% substrate concentration, coinciding with the maximum COD removal efficiency (45.13%). Even at 50% concentration, this ratio maintained substantial activity (54.6%) with 32.26% COD reduction.

Further increases in the C:N ratio (30:1 and 35:1) resulted in negligible antifungal activity (<5%), suggesting that nitrogen limitation beyond an optimal threshold adversely affects metabolite biosynthesis. These results demonstrate that a balanced C:N ratio is critical for triggering secondary metabolism in strain RM-1-138. The optimal condition (25:1 at 25% concentration) provided maximal antifungal activity alongside efficient substrate utilization, and was therefore selected for subsequent experiments.

3.6. Effect of seed inoculum size of S. philanthi RM-1-138 on antifungal metabolite production against S. commune

The effect of inoculum size of *S. philanthi* RM-1-138 on antifungal metabolite production and COD removal is shown in Fig. 3. In the untreated control, *S. commune* exhibited normal growth with a biomass of 80.33 mg (Fig. 3A). Increasing inoculum size significantly reduced fungal growth (one-way ANOVA, $F_{5,12} = 3629.79$, $p < 0.001$) and significantly enhanced mycelial growth inhibition (one-way ANOVA, $F_{4,10} = 1068.77$, $p < 0.001$). At 1% inoculum, inhibition was 39.0%, increasing to 66.1% at 2%, and reaching strong suppression at 5% (93.5%) and 10% (95.4%). Maximum inhibition (99.3%) was achieved at 15%, where fungal growth was nearly completely suppressed (Fig. 3B). COD removal was significantly affected by inoculum size (one-way ANOVA, $F_{4,10} = 4.861$, $p = 0.019$), increasing from 35.76% at 1% inoculum to 52.65% at 15% inoculum (Fig. 3C). The highest COD reduction at 15% inoculum indicates that higher cell density enhances both antifungal metabolite production and substrate utilization.

3.7. Effect of different concentrations of S. philanthi RM-1-138 culture filtrates on the inhibition of S. commune

The effects of different concentrations (1–60% v/v) of *S. philanthi* RM-1-138 CFs on the radial growth and growth inhibition of *S. commune* differed significantly among treatments (one-way ANOVA, radial growth: $F_{5,12} = 45.142$, $p < 0.001$; growth inhibition: $F_{4,10} = 424.329$, $p < 0.001$), as summarized in Table 4. The radial growth in the control was 9.00 cm. At 1% CFs, growth was slightly inhibited (8.84 cm; 1.82% inhibition). Increasing the concentration to 15%, 30%, 45%, and 60% progressively reduced fungal growth, resulting in inhibition rates of 26.7%, 58.9%, 72.7%, and 89.9%, respectively. These results clearly demonstrate a dose-dependent antifungal effect of RM-1-138 CFs against *S. commune*.

3.8. Comparative evaluation of the in vitro antifungal efficacy of S. philanthi RM-1-138 culture filtrates and commercial fungicides

The comparative antifungal efficacy of *S. philanthi* RM-1-138 CFs and commercial fungicides against *S. commune* is shown in Fig. 4. Significant differences in fungal radial growth (one-way ANOVA, $F_{13,28} = 432.738$, $p < 0.001$) and mycelial growth inhibition (one-way ANOVA, $F_{12,26} = 285.735$, $p < 0.001$) were observed among treatments. The untreated control exhibited the highest radial growth (8.50 cm) (Fig. 4A). In contrast, RM-1-138 CFs reduced growth to 2.46 cm, corresponding to 70.98% inhibition (Fig. 4B). This level of inhibition was comparable to thiram (73.13%) and pyraclostrobin (72.74%), as well as prochloraz and chlorothalonil + azoxystrobin (Fig. 4B). Propiconazole and copper hydroxide completely inhibited fungal growth (100%), while difenoconazole + propiconazole, fosetyl-aluminium, and mancozeb showed higher efficacy than RM-1-138 CFs (Fig. 4B). Conversely, azoxystrobin, metalaxyl, and carbendazim exhibited low to moderate antifungal activity (Fig. 4B). Colony morphology also differed among treatments, with clear suppression of mycelial development observed in RM-1-138 CFs and highly effective fungicides (Fig. 4C). Overall, RM-1-138 CFs demonstrated strong antifungal activity comparable to several commercial fungicides.

3.9. Antifungal activity of S. philanthi RM-1-138 culture filtrates against multiple plant pathogenic fungi

The culture filtrates of *S. philanthi* RM-1-138 produced in the optimized medium exhibited significantly different antifungal activities against nine phytopathogenic fungi (one-way ANOVA, $F_{8,18} = 283.120$, $p < 0.001$) (Fig. 5). Inhibition ranged from 45.8% to 81.8%, depending on the pathogen. The strongest effects were observed against *A. flavus* (81.8%) and *A. parasiticus* (74.0%). Moderate inhibition was recorded against *C. oryzae* (61.9%) and *S. rolfsii* (60.0%), whereas lower activity was found against *L. theobromae*, *P. salaccae*, *F. incarnatum*, *C. cassiicola*, and *R. solani* (45.8–56.3%) (Fig. 5). These results indicate that RM-1-138 metabolites exhibit differential antifungal activity against a range of phytopathogenic fungi, with particularly strong efficacy against

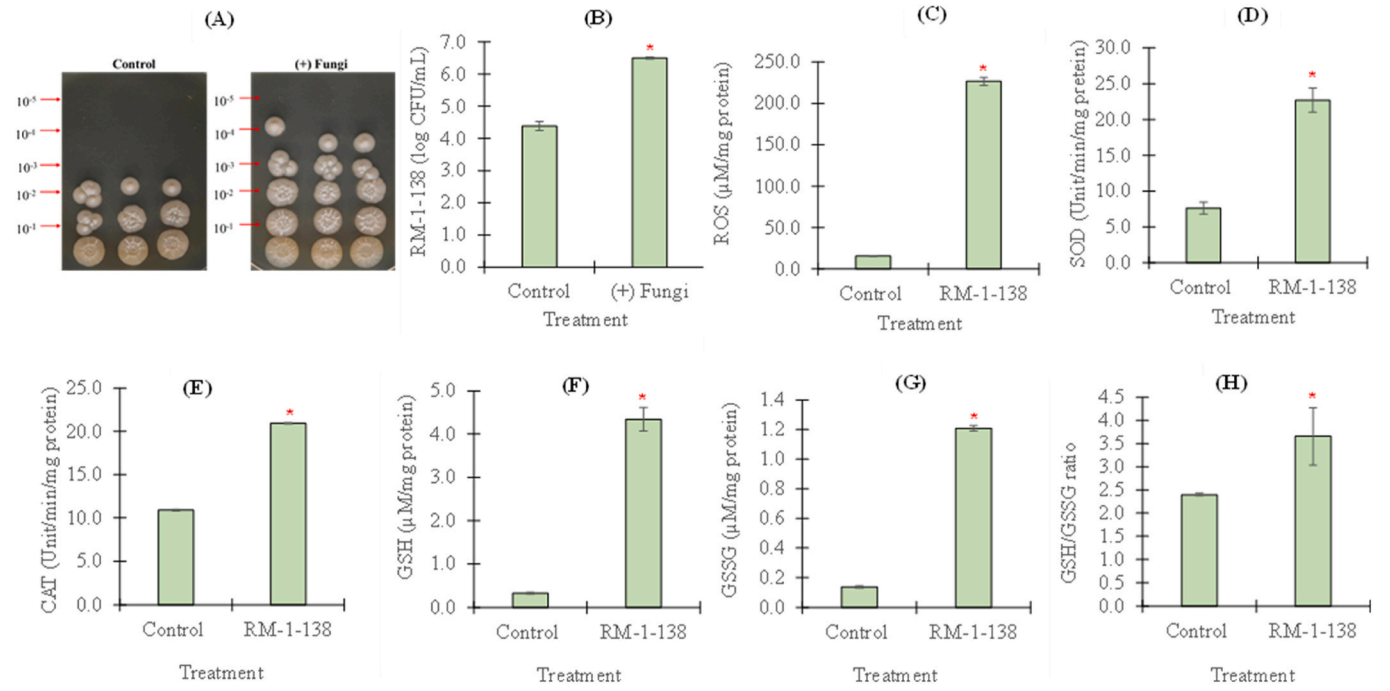

Fig. 7. *In vitro* mycolytic assay and the antifungal mechanism of *S. philanthi* RM-1-138 against *S. commune*. **(A, B)** Mycolytic assay; **(C)** intracellular reactive oxygen species (ROS) levels; **(D)** superoxide dismutase (SOD) activity; **(E)** catalase (CAT) activity; **(F)** reduced glutathione (GSH) levels; **(G)** oxidized glutathione (GSSG) levels; and **(H)** GSH/GSSG ratio. Data are presented as mean ± SD (n = 3). An asterisk (*) indicates a significant difference between the treated and untreated control groups (independent-samples *t*-test, $p < 0.05$).

Aspergillus species.

3.10. Comparative assessment of S. philanthi RM-1-138 culture filtrates and commercial fungicides against S. commune infection in an oil palm seed model

The disease incidence (Fig. 6A) and control efficacy (Fig. 6B) of *S. philanthi* RM-1-138 CFs and selected fungicides against *S. commune* in germinated oil palm seeds are shown in Fig. 6. Disease incidence (one-way ANOVA, $F_{5,12} = 415.865$, $p < 0.001$) and disease control efficacy (one-way ANOVA, $F_{4,10} = 105.703$, $p < 0.001$) differed significantly among treatments. The untreated control exhibited the highest disease incidence (76.56%). RM-1-138 CFs reduced disease incidence to 39.2%, corresponding to 48.8% disease control. Propiconazole and copper hydroxide showed the greatest efficacy, with disease incidences of 23.45% and 25.23% and control levels of 69.38% and 67.08%, respectively. Mancozeb and difenoconazole + propiconazole provided moderate control (60.97% and 57.05%). Overall, RM-1-138 CFs effectively reduced disease incidence, although their efficacy was lower than that of propiconazole and copper hydroxide and comparable to those of mancozeb and difenoconazole + propiconazole.

3.11. LC–QTOF–MS-based metabolite profiling of culture filtrates of S. philanthi RM-1-138

LC–QTOF–MS analysis was performed to profile secondary metabolites in culture filtrates of *S. philanthi* RM-1-138 grown under optimized conditions for 10 days. Analyses in both negative (−ESI) and positive (+ESI) ionization modes revealed a diverse metabolite profile (Tables S2 and S3, Supplementary Data). All compounds were considered putatively identified (MSI level 2–3) based on accurate mass, isotopic patterns, and database matching without confirmation using authentic standards or MS/MS validation.

In negative ionization mode (−ESI), a total of 66 metabolites were putatively identified, mainly comprising amino acids, small peptides, organic acids, nucleosides, and other primary metabolites. Notably, bioactive compounds such as natamycin and toyocamycin were detected, along with several diketopiperazines and amino acid derivatives, indicating that this mode favored the detection of polar and low molecular weight compounds.

In positive ionization mode (+ESI), 94 putatively annotated metabolites were detected, including amino acids and peptides, alkaloids, lipid-related compounds, and polyketide-associated metabolites. Anisomycin was among the bioactive compounds identified in this mode, together with various secondary metabolite-related structures, suggesting enhanced detection of a wider range of ionizable metabolites.

Comparison between the two ionization modes indicated partial overlap in metabolite classes, particularly amino acids, peptides, and nucleoside-related compounds, while each mode also exhibited distinct metabolite coverage. The −ESI mode preferentially detected acidic and polar metabolites, whereas the +ESI mode enabled detection of a broader range of structurally diverse compounds. Importantly, natamycin was detected only in −ESI, whereas anisomycin was observed only in +ESI, highlighting complementary ionization behavior between the two analytical conditions.

3.12. Mycolytic assay and interaction analysis of S. philanthi RM-1-138 against S. commune

3.12.1. Mycolytic assay

The population density of *S. philanthi* RM-1-138 increased in the presence of *S. commune* mycelia (Fig. 7A and B). The bacterial population reached 4.39 log CFU/mL in the absence of fungal biomass, whereas co-incubation resulted in a significantly higher density of 6.50 log CFU/mL (>2 log increase).

3.12.2. Oxidative stress–related assays

Exposure to *S. philanthi* RM-1-138 resulted in increased intracellular ROS levels in *S. commune* compared with the control (Fig. 7C–H). Activities of antioxidant enzymes, including SOD and CAT, were also

significantly altered. In addition, changes in the glutathione redox system (GSH and GSSG levels) were observed in treated samples relative to the control.

4. Discussion

Nutrient-rich agro-industrial waste streams such as POME and tuna condensate are promising resources for sustainable microbial valorization. The present study demonstrates that the combined use of these substrates supports the growth of *S. philanthi* RM-1-138 and stimulates the biosynthesis of antifungal metabolites, highlighting dual benefits for environmental management and agricultural applications [1–6,10]. Physicochemical variability of waste streams, influenced by seasonal and processing factors, emphasizes the importance of substrate characterization prior to fermentation [30,31]. The complementary nutrient composition of carbon-rich POME and nitrogen-rich tuna condensate establishes a favorable C:N ratio that promotes secondary metabolism, consistent with previous observations in waste-based *S. philanthi* cultures [10,32].

The LC–QTOF–MS-based metabolite profiling revealed a diverse spectrum of putatively annotated metabolites, mainly comprising amino acids, peptides, diketopiperazines, nucleoside- and purine-related compounds, and lipid-derived metabolites. These annotations were based on accurate mass and spectral database matching and should be considered putative (MSI level 2–3) [33]. Genome mining using antiSMASH further revealed multiple biosynthetic gene clusters (BGCs), including NRPS, PKS, terpene, and lanthipeptide-related pathways, indicating a broad biosynthetic potential of *S. philanthi* RM-1-138 [34]. Notably, a NRPS-associated cluster showed similarity to a bacillibactin-like siderophore biosynthetic pathway, suggesting a potential capacity for iron acquisition. Although several metabolite classes detected by LC–QTOF–MS are generally consistent with the predicted genomic potential, the link between detected metabolites and specific BGCs remains putative and requires further experimental validation [35,36].

Mechanistic interpretation indicates that RM-1-138 exhibits multifactorial antifungal activity. Polyene- and polyketide-related metabolites, such as natamycin, are likely to affect fungal membrane integrity through sterol interactions [37,38]. Translation-inhibiting compounds such as anisomycin and nucleoside analogues may contribute to suppression of fungal growth [39]. In addition, oxidative stress–related responses observed in *S. commune*, including increased ROS accumulation and alterations in antioxidant enzymes (SOD and CAT) as well as glutathione redox balance, suggest a physiological stress response rather than a confirmed mechanistic pathway. Although oxidative stress–related parameters indicate physiological stress in *S. commune*, these results should be interpreted as associative evidence rather than direct confirmation of a specific killing mechanism.

Furthermore, the increased bacterial population in the presence of fungal biomass observed in the co-culture assay suggests a possible utilization of fungal-derived nutrients under interaction conditions, based on indirect growth-based evidence. Direct microscopic or enzymatic validation was not performed. In addition, the proposed mechanisms, including oxidative stress induction and putative mycolytic activity, are inferred from physiological responses and require direct microscopic, molecular, and genetic validation.

Optimization of cultivation parameters, including C:N ratio, substrate dilution, and inoculum size, was shown to influence secondary metabolism and antifungal efficacy, consistent with *Streptomyces* physiology and previous studies linking nutrient balance to metabolite production [40–42]. Collectively, these findings suggest a multifactorial mode of antifungal activity involving membrane disruption, metabolic interference, oxidative stress responses, iron competition, and possible nutrient utilization from fungal biomass. However, it should be noted that this study was conducted under controlled laboratory conditions using a seed-based assay, which does not fully represent field conditions. Although the culture filtrates significantly reduced disease severity compared with the untreated control, the level of disease suppression should be considered a preliminary indication of efficacy under laboratory conditions rather than evidence of field performance. Therefore, further validation under greenhouse and field conditions is required to confirm its practical applicability.

The integration of genome mining and metabolite profiling provides a framework for understanding the functional potential of RM-1-138 in waste-based systems. By converting agro-industrial by-products into bioactive metabolites, RM-1-138 represents a genome-informed and metabolite-guided biocontrol candidate suitable for sustainable disease management. Limitations include the reliance on putative metabolite annotation without validation using authentic standards and the absence of direct functional linkage between specific biosynthetic gene clusters and individual metabolites. Future work involving targeted metabolite isolation, gene expression analysis, and genetic validation is needed to confirm these mechanistic relationships.

5. Conclusion

This study demonstrates the feasibility of a waste-to-antifungal bioprocess using *S. philanthi* RM-1-138 to convert palm oil mill effluent and tuna condensate into bioactive antifungal metabolites. Strong inhibition of *S. commune* was observed, while comparative genome mining and LC–QTOF–MS-based metabolite profiling provided complementary (rather than causally linked) insights into the biosynthetic potential and chemical diversity of the strain. Multiple biosynthetic gene clusters were identified alongside a chemically diverse repertoire of putatively annotated metabolites detected by LC–QTOF–MS. Mechanistic analyses suggest a multifactorial mode of antifungal action, including oxidative stress induction, disruption of fungal antioxidant responses, and possible fungal biomass utilization. The latter is inferred from indirect evidence and should be interpreted cautiously as a putative mycolytic-like interaction. Collectively, these findings highlight the potential of integrating microbial secondary metabolism with agro-industrial waste valorization, providing a genome-informed and metabolite-guided framework for the development of sustainable antifungal bioprocesses and value-added products. Further studies involving targeted metabolite validation and genetic confirmation are warranted to substantiate these mechanistic hypotheses.

Funding

This research was financially supported by the Fundamental Fund (FF, Grant No. 1/2568) and the National Research Council of Thailand (NRCT, Grant No. N42A680491).

CRediT authorship contribution statement

Wanida Petlamul: Conceptualization, Data curation, Formal analysis, Investigation, Writing – original draft, Writing – review & editing. **Sawai Boukaew:** Conceptualization, Data curation, Formal analysis, Funding acquisition, Investigation, Methodology, Project administration, Resources, Software, Supervision, Validation, Visualization, Writing – original draft, Writing – review & editing. **Benjamas Cheirsilp:** Funding acquisition, Writing – review & editing. **Siriporn Yossan:** Data curation, Formal analysis, Writing – review & editing. **Kanokphorn Sangkharak:** Data curation, Formal analysis, Writing – review & editing.

Declaration of competing interest

The authors declare that they have no conflicts of interest, financial or personal, that could have inappropriately influenced the work reported in this study.

Appendix A. Supplementary data

Supplementary data to this article can be found online at https://doi.org/10.1016/j.pmpp.2026.103441.

Data availability

Data will be made available on request.

References

[1] B. Nurul-Adela, A.B. Nasrin, S.K. Loh, Palm oil mill effluent as a low-cost substrate for bioflocculant production by *Bacillus marisflavi* NA8, Bioresour. Bioprocess. 3 (2016) 20, https://doi.org/10.1186/s40643-016-0096-6.

[2] A.L. Ahmad, S. Ismail, S. Bhatia, Water recycling from palm oil mill effluent (POME) using membrane technology, Desalination 157 (2003) 87–95.

[3] Y.M. Tang, K.T. Tan, L.P. Wong, Palm oil mill effluent (POME) as a source of biofuels and value-added products via oil recovery: a review, J. Oil Palm Res. 36 (2024) 534–546, https://doi.org/10.21894/jopr.2023.0056.

[4] Q.N. Ho, W.J. Lau, J. Jaafar, M.H.D. Othman, N. Yoshida, Membrane technology for valuable resource recovery from palm oil mill effluent (POME): a review, Membranes 15 (2025) 138, https://doi.org/10.3390/membranes15050138.

[5] A.E. Ghaly, V.V. Ramakrishnan, M.S. Brooks, S.M. Budge, D. Dave, Fish processing wastes as a potential source of proteins, amino acids and oils: a critical review, J. Microb. Biochem. Technol. 5 (2013) 107–129, https://doi.org/10.4172/1948-5948.1000110.

[6] V. Šimat, Valorization of seafood processing by-products, in: R. Bhat (Ed.), Valorization of Agri-Food Wastes and By-Products: Recent Trends, Innovations and Sustainability Challenges, Academic Press, 2021, pp. 515–536, https://doi.org/10.1016/B978-0-12-824044-1.00017-9.

[7] J.R. Doroghazi, W.W. Metcalf, Comparative genomics of actinomycetes with a focus on natural product biosynthetic genes, BMC Genom. 11 (2013) 611, https://doi.org/10.1186/1471-2164-14-611.

[8] M.H. Medema, R. Kottmann, P. Yilmaz, et al., Minimum information about a biosynthetic gene cluster, Nat. Chem. Biol. 11 (2015) 625–631, https://doi.org/10.1038/nchembio.1890.

[9] S. Boukaew, W. Petlamul, P. Prasertsan, Tuna condensate waste with molasses as a renewable substrate for antifungal compounds by *Streptomyces philanthi* RL-1-178 against aflatoxingenic B1 (AFB1) *Aspergillus flavus*, Waste Biomass Valor. 11 (2020) 1321–1331, https://doi.org/10.1007/s12649-018-0530-4.

[10] S. Boukaew, B. Cheirsilp, S. Yossan, U. Khunjan, W. Petlamul, P. Prasertsan, Utilization of palm oil mill effluent as a novel substrate for the production of antifungal compounds by *Streptomyces philanthi* RM-1-138 and evaluation of its efficacy in suppression of three strains of oil palm pathogen, J. Appl. Microbiol. 132 (2022) 1990–2003, https://doi.org/10.1111/jam.15304.

[11] S. Boukaew, P. Prasertsan, W. Petlamul, B. Cheirsilp, Palm oil decanter cake wastes as alternative nutrient sources for production of enzymes from *Streptomyces philanthi* RM-1-138 and the efficacy of its culture filtrate as an antimicrobial agent against plant pathogenic fungi and bacteria, Biomass Convers. Biorefinery 14 (2024) 1895–1904, https://doi.org/10.1007/s13399-022-02448-7.

[12] A. Dikin, K. Sijam, Z.A.M. Ahmad, I.A. Seman, Biological control of seedborne pathogen of oil palm, *Schizophyllum commune* Fr., with antagonistic bacteria, Int. J. Agric. Biol. 5 (2003) 507–512.

[13] S. Boukaew, S. Chuenchit, V. Petcharat, Evaluation of *Streptomyces* spp. for biological control of *Sclerotium* root and stem rot and *Ralstonia* wilt of chili pepper, BioControl 56 (2011) 365–374, https://doi.org/10.1007/s10526-010-9336-4.

[14] W. Petlamul, J. Buatong, K. Nooprom, B. Cheirsilp, S. Srinuanpan, K. Chumkaew, S. Yossan, S. Chankaew, A. Chumthong, S. Boukaew, Biocontrol potential of *Trichoderma* culture filtrates against *Schizophyllum commune*: metabolite profiling and oxidative stress mechanisms, Physiol. Mol. Plant Pathol. (2026) 103195, https://doi.org/10.1016/j.pmpp.2026.103195.

[15] J. Chuprom, S. Boukaew, W. Petlamul, M. Kaewnah, O. Pora, J. Buatong, B. Cheirsilp, S. Yossan, K. Sangkharak, L. Khwanchum, Z. Zhang, A sustainable biocontrol strategy using *Priestia aryabhattai* C-KT-3 to manage postharvest nutmeg black rot caused by *Lasiodiplodia theobromae*, Food Control 189 (2026) 112334, https://doi.org/10.1016/j.foodcont.2026.112334.

[16] S. Boukaew, J. Kumla, N. Suwannarach, *Peniophora salaccae* sp. Nov. (Russulales, Basidiomycota), a snake fruit (*Salacca zalacca*) pathogen from southern Thailand, Phytotaxa 662 (2024) 137–149, https://doi.org/10.11646/phytotaxa.662.2.2.

[17] APHA, Standard Methods for the Examination of Water and Waste Water, twenty-second ed., American Public Health Association, American Water Works Association, Water Environment Federation, Washington, DC, 2012.

[18] T. Nutongkaew, P. Prasertsan, C. Leamdum, S. Sattayasamitsathit, P. Noparat, Bioconversion of oil palm trunk residues hydrolyzed by enzymes from newly isolated fungi and use for ethanol and acetic acid production under two-stage and simultaneous fermentation, Waste Biomass Valor. 11 (2020) 1333–1347, https://doi.org/10.1007/s12649-019-00678-x.

[19] R.R. Wick, L.M. Judd, C.L. Gorrie, K.E. Holt, Unicycler: resolving bacterial genome assemblies from short and long sequencing reads, PLoS Comput. Biol. 13 (2017) e1005595, https://doi.org/10.1371/journal.pcbi.1005595.

[20] T. Seemann, Prokka: rapid prokaryotic genome annotation, Bioinformatics 30 (2014) 2068–2069, https://doi.org/10.1093/bioinformatics/btu153.

[21] M. Mannaa, T. Jung, A. Kim, D. Lee, Y.-S. Seo, Characterization of *Lasiodiplodia brasiliensis* causing banana black rot in Korea and its biocontrol by *Paraburkholderia busanensis* P39 through volatile-mediated microbiome modulation, Postharvest Biol. Technol. 227 (2025) 113621, https://doi.org/10.1016/j.postharvbio.2025.113621.

[22] M. Mannaa, G. Han, T. Jeong, M. Kang, D. Lee, H. Jung, Y.-S. Seo, Taxonomy-guided selection of *Paraburkholderia busanensis* sp. Nov.: a versatile biocontrol agent with mycophagy against *Colletotrichum scovillei* causing pepper anthracnose, Microbiol. Spectr. 11 (2023) e02426–23, https://doi.org/10.1128/spectrum.02426-23.

[23] H. Yaakoub, S. Mina, A. Calenda, J.-P. Bouchara, N. Papon, Oxidative stress response pathways in fungi, Cell. Mol. Life Sci. 79 (2022) 333, https://doi.org/10.1007/s00018-022-04353-8.

[24] J. Park, H. Son, Antioxidant systems of plant pathogenic fungi: functions in oxidative stress response and their regulatory mechanisms, Plant Pathol. J. 40 (2024) 235–250, https://doi.org/10.5423/PPJ.RW.01.2024.0001.

[25] A.S. Keston, R. Brandt, The fluorometric analysis of ultramicro quantities of hydrogen peroxide, Anal. Biochem. 11 (1965) 1–5, https://doi.org/10.1016/0003-2697(65)90034-5.

[26] S. Das, V.K. Singh, A.K. Dwivedy, A.K. Chaudhari, N.K. Dubey, *Myristica fragrans* essential oil nanoemulsion as novel green preservative against fungal and aflatoxin contamination of food commodities with emphasis on biochemical mode of action and molecular docking of major components, LWT Food Sci. Technol. 130 (2020) 109495, https://doi.org/10.1016/j.lwt.2020.109495.

[27] R.F. Beers, I.W. Sizer, A spectrophotometric method for measuring the breakdown of hydrogen peroxide by catalase, J. Biol. Chem. 195 (1952) 133–140.

[28] V.A. Kostyuk, A.I. Potapovich, Superoxide-driven oxidation of quercetin and a simple sensitive assay for determination of superoxide dismutase, Biochem. Int. 19 (1989) 1117–1124.

[29] O.H. Lowry, N.J. Rosebrough, A.L. Farr, R.J. Randall, Protein measurement with the Folin phenol reagent, J. Biol. Chem. 193 (1951) 265–275.

[30] S.Z.Y. Foong, M.F. Chong, D.K.S. Ng, Strategies to promote biogas generation and utilisation from palm oil mill effluent, Process Integr. Optim. Sustain. 5 (2021) 175–191, https://doi.org/10.1007/s41660-020-00121-y.

[31] R. Karno, H. Susanto, M. Nur, H.H. Diantoro, D. Siswanto, Physicochemical properties of wastewater from palm oil mill secondary effluent (POMSE) for water evaluation quality, BIO Web Conf. 117 (2024) 01039, https://doi.org/10.1051/bioconf/202411701039.

[32] K. Sangkharak, N. Paichid, T. Yunu, S. Klomklao, P. Prasertsan, Utilisation of tuna condensate waste from the canning industry as a novel substrate for polyhydroxyalkanoate production, Biomass Convers. Biorefinery 11 (2021) 2053–2064, https://doi.org/10.1007/s13399-019-00581-4.

[33] R. Chaleckis, I. Meister, P. Zhang, C.E. Wheelock, Challenges, progress and promises of metabolite annotation for LC-MS-based metabolomics, Curr. Opin. Biotechnol. 55 (2019) 44–50, https://doi.org/10.1016/j.copbio.2018.07.010.

[34] K. Blin, H.U. Kim, M.H. Medema, T. Weber, Recent development of antiSMASH and other computational approaches to mine secondary metabolite biosynthetic gene clusters, Briefings Bioinf. 19 (2019) 1103–1113, https://doi.org/10.1093/bib/bbx146.

[35] S. Soldatou, G.H. Eldjarn, A. Huerta-Uribe, S. Rogers, K.R. Duncan, Linking biosynthetic and chemical space to accelerate microbial secondary metabolite discovery, FEMS Microbiol. Lett. 366 (2019), https://doi.org/10.1093/femsle/fnz142.

[36] J.J.R. Louwen, M.H. Medema, J.J.J. van der Hooft, Enhanced correlation-based linking of biosynthetic gene clusters to their metabolic products through chemical class matching, Microbiome 11 (2023) 13, https://doi.org/10.1186/s40168-022-01444-3.

[37] Y.M. te Welscher, H.H. ten Napel, M.M. Balagué, C.M. Souza, H. Riezman, B. de Kruijff, E. Breukink, Natamycin blocks fungal growth by binding specifically to ergosterol without permeabilizing the membrane, J. Biol. Chem. 283 (2008) 6393–6401, https://doi.org/10.1074/jbc.M707821200.

[38] Y.M. te Welscher, L. Jones, M.R. van Leeuwen, J. Dijksterhuis, B. de Kruijff, G. Eitzen, E. Breukink, Natamycin inhibits vacuole fusion at the priming phase via a specific interaction with ergosterol, Antimicrob. Agents Chemother. 54 (2010) 2618–2625, https://doi.org/10.1128/AAC.01794-09.

[39] U. Frey, M. Krug, K.G. Reymann, H. Matthies, Anisomycin, an inhibitor of protein synthesis, blocks late phases of LTP phenomena in the hippocampal CA1 region in vitro, Brain Res. 452 (1988) 57–65, https://doi.org/10.1016/0006-8993(88)90008-x.

[40] T. Egli, J.R. Quayle, Influence of the carbon:nitrogen ratio of the growth medium on the cellular composition and the ability of the methylotrophic yeast *Hansenula polymorpha* to utilize mixed carbon sources, J. Gen. Microbiol. 132 (1986) 1779–1788.

[41] J.V. Moreira, S.C.M. Silva, M.A. Cremasco, Evaluation of carbon:nitrogen ratio in semi-defined culture medium to tacrolimus biosynthesis by *Streptomyces tsukubaensis* and the effect on bacterial growth, Biotechnol. Rep. 26 (2020) e00440, https://doi.org/10.1016/j.btre.2020.e00440.

[42] S.B. Ferraiuolo, M. Cammarota, C. Schiraldi, O.F. Restaino, *Streptomycetes* as platform for biotechnological production processes of drugs, Appl. Microbiol. Biotechnol. 105 (2021) 551–568, https://doi.org/10.1007/s00253-020-11064-2.